

FIG. 2. Arrhenius plot for self-diffusion in Zr. Open circles are data of Federer and Lundy (Ref. 16); solid line represents the fitted equation (5).

have the expected magnitudes, and the fit to available data is as close as can be. Although the present model applies strictly to Ti, Zr, and Hf, where the metastable ω phase has been reported, the authors believe that a similar mechanism should apply to the other anomalous bcc metals, the only requirement being the tendency to form trigonal bonds on a (111) plane, as in the ω structure. Further work, both theoretical and experimental, is needed to elucidate this point. A cluster-variation study of the temperature dependence of the concentration of ω embryos above T_0 is in progress.

¹A. D. LeClaire, in *Proceedings of a Conference on Diffusion in Body-Centered Cubic Metals*, Gatlinburg, Tennessee, 1964 (American Society for Metals, Metals Park, Ohio, 1965), p. 3.

²S. J. Rothman and N. L. Peterson, in *Proceedings of a Conference on Diffusion in Body-Centered Cubic Metals*, Gatlinburg, Tennessee, 1964 (American Society for Metals, Metals Park, Ohio, 1965), p. 183.

³N. L. Peterson, in *Proceedings of the Conference on the Local Structural Order and Decomposition of Titanium, Uranium, and Zirconium-Based Body-Centered Cubic Solid Solutions*, Cornell University, Ithaca, New York, May 1972 (unpublished).

⁴A. Seeger, *J. Less-Common Metals* **28**, 38 (1972).

⁵G. V. Kidson, *Can. J. Phys.* **41**, 1563 (1963).

⁶H. I. Aaronson and P. G. Shewmon, *Acta Met.* **15**, 385 1676 (1967).

⁷J. E. Doherty and D. F. Gibbons, *Acta Met.* **19**, 275 (1971).

⁸D. de Fontaine and Otto Buck, *Philos. Mag.* **27**, 967 (1973).

⁹J. M. Silcock, H. M. Davies, and H. K. Hardy, *Mechanism of Phase Transformations in Metals*, Monograph and Report Series No. 18 (Institute of Metals, London, 1956), p. 93.

¹⁰J. D. Jamieson, *Science* **140**, 72 (1963).

¹¹C. Wert and C. Zener, *Phys. Rev.* **76**, 1169 (1949).

¹²S. C. Moss, D. T. Keating, and J. D. Axe, *Mater. Res. Bull.* **9**, 179 (1973).

¹³K. K. McCabe and S. L. Sass, *Philos. Mag.* **23**, 957 (1971).

¹⁴D. de Fontaine, N. E. Paton, and J. C. Williams, *Acta Met.* **19**, 1153 (1971).

¹⁵H. E. Cook, *Acta Met.* **21**, 1431 (1973).

¹⁶D. J. Cometto, G. L. Houze, Jr., and R. F. Hehemann, *Trans. AIME* **223**, 30 (1965).

¹⁷J. I. Federer and T. S. Lundy, *Trans. AIME* **227**, 592 (1963).

¹⁸J. M. Sanchez and D. de Fontaine, to be published.

X-Ray-Diffraction Studies of Acoustoelectrically Amplified Phonon Beams*

S. D. LeRoux, R. Colella, and R. Bray

Physics Department, Purdue University, West Lafayette, Indiana 47907

(Received 19 May 1975)

Highly resolved satellite peaks due to acoustoelectrically amplified phonons are observed on the wings of double-crystal x-ray diffraction peaks in InSb single crystals. The frequencies of the observed phonon peaks range between 0.9 and 6.3 GHz, depending on carrier concentration. Second- and third-order satellites are also visible in all profiles, showing the generation of second and third harmonics of the fundamental frequencies of the amplified phonons and, possibly, the existence of multiphonon scattering.

An intense field of quasi monochromatic acoustic phonons with well-defined directions of propagation and polarization can be produced in piezoelectric semiconductors by acoustoelectric (AE)

amplification of phonons from the thermal-equilibrium background. The characteristics^{1,2} of such amplified phonon beams at frequencies below ≈ 5 GHz have been analyzed intensively in

GaAs and CdS by Brillouin scattering at optical wavelengths depending on the transparency of the materials. The extension of scattering studies from the optical to the x-ray region makes it possible to investigate much higher-frequency phonons and to study AE phonons in a greater variety of materials, without regard to their optical transparency. Thus we are able to describe here the first such scattering experiments in InSb. The fact that InSb is opaque at wavelengths below $\approx 6.0 \mu\text{m}$ has discouraged any investigations by optical Brillouin scattering.

The dynamical³ and kinematic⁴ theories of the interaction of x rays with phonons both predict that phonons with a single wave vector \vec{g} produce a set of satellites symmetrically located with respect to each elastic x-ray reflection, at a distance from the associated node in reciprocal space equal to $n\vec{g}$ ($n = 1, 2, \dots$). The diffuse tails accompanying ordinary Bragg reflections are a manifestation of the total thermal phonon background always present in a crystal. The use of AE amplification provides an opportunity to study the details of the interaction of phonons with x rays under controlled conditions of phonon frequency and propagation and polarization directions.

Results of x-ray-scattering experiments with AE phonons have been reported recently for CdS⁵ and epitaxial GaAs^{6,7} samples. These studies were made at relatively low resolution and thus revealed only a broadening of the x-ray diffraction profiles. The satellite profiles (attributable to the annihilation and creation of phonons) were obtained by subtracting the undisturbed profile obtained without AE phonons. However, when the satellites are not resolved from the Bragg elastic peak, the diffraction profile is the result of multibeam diffraction,³ and the physical meaning of subtracting the undisturbed profile is not clear. Furthermore, the subtraction procedure ignores the possible effect of the phonons on the elastic Bragg peaks themselves.

In this paper we report a high-resolution, double-crystal-spectrometer study, which provides the first observation of phonon-generated x-ray satellites completely resolved from the Bragg elastic peak, even for phonon frequencies as low as 1 GHz. Thus we can not only determine the phonon spectrum more accurately, but we can observe possible effects of the phonons on the elastic Bragg peaks.

InSb was chosen for our investigation, not only because of the absence of any optical-scattering

information, but because its electrical properties made it particularly favorable for x-ray-scattering experiments. From earlier electrical studies of AE amplification,⁸ it was known that in relatively pure *n*-InSb samples, immersed in liquid nitrogen, it is possible to achieve close to dc power input and obtain almost continuous phonon amplification. This removes the impediment of infrequent short-pulse operation required in other materials to avoid unduly heating the samples. The greatly enhanced duty cycle in InSb permits full x-ray scans in only 15–60 min. This favorable situation is achieved by applying a transverse magnetic field of a few kilogauss to samples with very high electron mobility, $\mu \geq 2 \times 10^5 \text{ cm}^2/\text{V sec}$. The magnetic field not only greatly enhances the acoustoelectric gain and permits effective phonon amplification at relatively low electric fields of a few tens of volts per centimeter, but the strong magnetoresistive effect helps reduce the associated power input to the sample. However, these factors employed to obtain high duty cycle restricted our measurements to samples of relatively low electron concentration, $n < 6 \times 10^{15} \text{ cm}^{-3}$. From AE theory,⁹ the phonon frequency f_m at which the AE gain is maximum at this carrier concentration is $< 10 \text{ GHz}$, with $f_m \propto n^{1/2}$. Thus our present study is restricted to relatively low frequencies.

The InSb samples were cut in the form of long, thin rectangular rods (typical dimensions: $23 \times 2 \times 1 \text{ mm}^3$) parallel to $[110]$ with one surface parallel to (001) . The amplified phonon beam consists of the piezoelectrically active fast transverse acoustic phonons propagating along the length of the sample, with atomic displacement along the $[001]$ direction. The crystals were ground, and then etched in CP4 for 3–5 sec. Thin copper wires were indium soldered to the ends of the rod. The samples were attached with one drop of varnish¹⁰ to a substrate of high-resistance, polycrystalline InSb to minimize strain due to differential thermal contraction when cooled to 77°K. Typical current and voltage pulses several hundred microseconds long are shown in Fig. 1. The current remains briefly at an initial Ohmic value (1 A), and then, after a few oscillations, drops to a reduced steady-state value. The voltage pulse shows the complementary increase. The high-resistance, steady-state condition represents the achievement of a stationary pattern of acoustic flux in the sample during most of the pulse duration. The maximum intensity is close to the positive end of the sample.¹¹

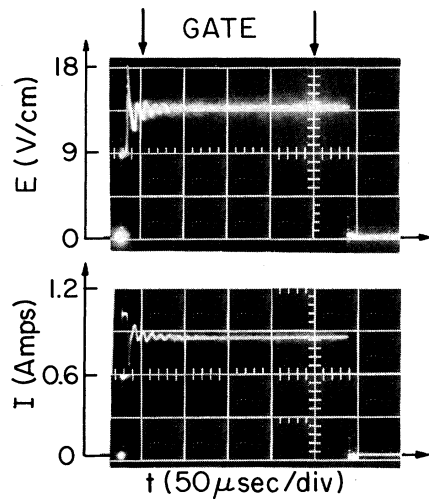


FIG. 1. Typical current and voltage pulses. After an initial Ohmic value, the building up of AE flux manifests itself through a series of damped oscillations. The steady-state regime is an indication of a stationary domain.

The x-ray spot projected on the surface of the sample is a line normal to $[110]$, 1 mm wide. For the x-ray-scattering studies, a double-crystal technique in the parallel arrangement ($n, -n$) was used. The cryostat, containing the sample immersed in liquid nitrogen, was rocked between the pole pieces of an electromagnet, and the 004 and 008 nodes were scanned along the $[110]$ direction. Use of hard x-ray radiation ($\text{Mo } K\alpha$; $\lambda = 0.711 \text{ \AA}$) kept absorption losses through the liquid nitrogen within tolerable limits. A full-wave-rectified x-ray generator provided 120 x-ray pulses/sec (typical working conditions were 43 kV and 25 mA) and electric pulses 2 msec long (or shorter) were fed to the sample every other x-ray pulse. A conventional detection system equipped with a proportional counter and a single-channel analyzer was gated in such a way that the output was connected to the first half of a multichannel scaler when the phonons were on and to the second half when the phonons were off. The address within each section of the multichannel scaler was advanced in synchronism with a motor that slowly rocked the second crystal through the Bragg peak. In this way profiles, both with and without phonons, were simultaneously recorded and drifting effects could be avoided.

Examples of profiles are reported in Fig. 2 for varying carrier concentration, voltage, and magnetic field, all for the 004 reflection. Figure 3

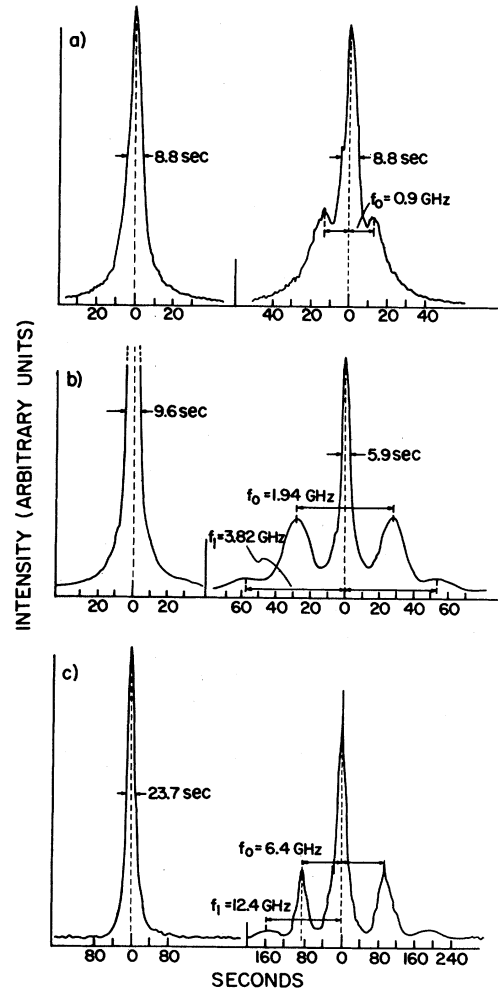


FIG. 2. Double-crystal 004 rocking curves of InSb single crystals, in presence (right-hand side) and absence (left-hand side) of AE phonons, at 77°K. Conditions: (a) $n = 5 \times 10^{13} / \text{cm}^3$; $\mu = 6 \times 10^5 \text{ cm}^2 / \text{V sec}$; $V = 60 \text{ V}$, $B = 4.5 \text{ kG}$. (b) $n = 3.5 \times 10^{14} / \text{cm}^3$; $\mu = 5 \times 10^5 \text{ cm}^2 / \text{V sec}$; $V = 20 \text{ V}$, $B = 5.1 \text{ kG}$. (c) $n = 5.5 \times 10^{15} / \text{cm}^3$; $\mu = 1.9 \times 10^5 \text{ cm}^2 / \text{V sec}$; $V = 25 \text{ V}$, $B = 14.3 \text{ kG}$.

shows an 008 reflection repeated for the purest sample, with greater resolution. In each figure, the unperturbed profile, without phonons, is shown on the left-hand side. Nearly perfect crystals could be selected whose Bragg linewidths were close to the theoretical value predicted by dynamical theory. Resolved phonon satellites are observed at 0.9, 1.94, and 6.4 GHz in the three samples of Fig. 2. The frequencies of the peaks are in fair agreement with the calculated values of frequency at maximum gain⁹ and show the expected increase with carrier concentration. The sample with the largest carrier concentra-

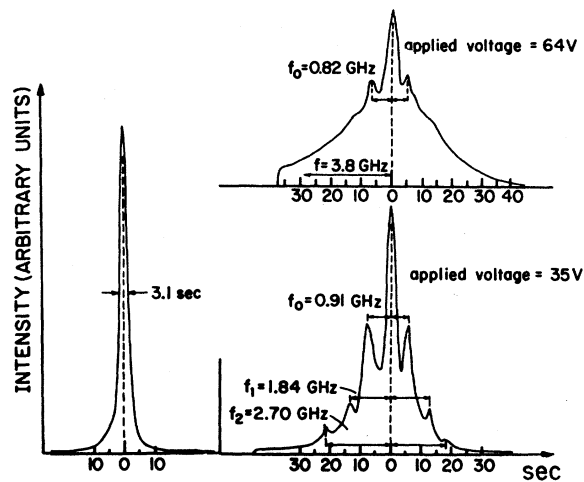


FIG. 3. Same as Fig. 2, except that the 008 reflection is presented. Conditions: $n = 5 \times 10^{13}/\text{cm}^3$; $\mu = 6 \times 10^5 \text{ cm}^2/\text{V sec}$; $B = 4.75 \text{ kG}$.

tion required special conditions. In order to obtain a sustained and sufficiently intense phonon flux it was necessary to use a stronger magnetic field (14.3 kG) and a thin sample ($25 \times 1 \times 0.4 \text{ mm}^3$). Also, shorter voltage pulses and wider x-ray slits were used, giving the broader linewidth shown in Fig. 2(c).

The dominant phonon satellites referred to above represent the first stage of phonon amplification governed by the "small-signal" AE theory.¹ Interesting additional structure is observed with increasing phonon intensity. Second- and third-order satellites appear, as is most clearly visible in Fig. 3, in the high-resolution 008 profile taken at an applied voltage of 35 V. It was observed that, with increasing voltage, the higher-order satellites continue to grow even after the first-order satellites tend to saturate. At still higher voltage (64 V in Fig. 3) there is a loss of structure, with a general broadening, producing a diffuse tail with much greater intensities at high frequencies. There is also a shift of the fundamental peak to lower frequency, and a broadening of the base of the Bragg peak (not shown here) suggesting a strong increase in very low-frequency phonons.

Most of these features have also been seen in recent, high-resolution optical Brillouin studies in GaAs,¹² and attributed to sum- and difference-phonon-frequency generation. The second and third "harmonics" of the fundamental peak correspond to the generation of sum frequencies from the interaction of all possible pairs of intense

acoustic waves near f_m . The ultimate loss of structure in the spectrum is a consequence of the downshift in frequency of the fundamental peak and the multiplicity of possible phonon interactions. Second-harmonic peaks due to sum-frequency generation have also been seen in the x-ray-scattering studies of very high-frequency phonons in degenerate, epitaxial GaAs.¹³ The interpretation of the structure of the intense phonon spectrum is consistent with the very strong nonlinear phonon-phonon interaction to be expected in piezoelectric semiconductors.^{12, 14} However, we cannot exclude some contribution to the observations from multiple-phonon x-ray scattering.

The effect of intense phonon scattering on the elastic central peaks is particularly noticeable in Fig. 2(b), where the height and the half-width are dramatically reduced. More generally we see mainly a reduction in height of the central peak. This corresponds to an enhanced Debye-Waller factor, and is reminiscent of the "thermal narrowing" of the Bragg peaks experimentally observed in silicon at high temperature.¹⁵

A rough estimate of the amplified phonon density can be extracted from the integrated intensities of the first-order satellites in the following manner. The theoretical treatment of dynamical diffraction in a vibrating, harmonic, otherwise perfect crystal³ shows that, when the first-order satellites are well resolved from the Bragg peak and from higher orders, they can be thought of as ordinary x-ray reflections whose structure factors are given by the product of the structure factor of the main reflection times a first-order Bessel function. The argument of such a function involves the scalar product between the reciprocal-lattice vector of the main reflection and the maximum amplitude of the phonon. By comparing the integrated intensity of the first-order satellite with the unperturbed Bragg peak, one can then evaluate the maximum vibrational amplitude, which, in a typical case [Fig. 2(b)] turns out to be 0.32 \AA . This displacement corresponds to an amplification factor of the order of 10^8 with respect to a Debye spectrum over the frequency range encompassed by each one of the first-order satellites as shown in Fig. 2(b). This value for the amplification factor is in fair agreement with evaluations from optical Brillouin-scattering studies¹ in GaAs.

*Research supported by the National Science Foundation—Materials Research Laboratory Program, Grant

No. GH 33574A1. One of the authors (S. D. LeRoux) is grateful to the South African Atomic Energy Board for partial support of his stay at Purdue University.

¹D. L. Spears, Phys. Rev. B 2, 1931 (1970); E. D. Palik and R. Bray, Phys. Rev. B 3, 3302 (1971).

²M. Yamada, C. Hamaguchi, K. Matsumoto, and J. Nakai, Phys. Rev. B 7, 2682 (1973); U. Gelbart and A. Many, Phys. Rev. B 7, 2713 (1973).

³R. Köhler, W. Möhling, and H. Peibst, Phys. Status Solidi 41, 75 (1970).

⁴B. E. Warren, *X-Ray Diffraction* (Addison-Wesley, Reading, Mass., 1969), Chap. 11.

⁵R. Köhler, W. Möhling, and H. Peibst, Phys. Status Solidi (b) 61, 439 (1974).

⁶D. G. Carlson, A. Segmüller, E. Mosekilde, H. Cole, and J. A. Armstrong, Appl. Phys. Lett. 18, 330 (1971).

⁷T. Ishibashi, M. Kitamura, and A. Odajima, Phys. Lett. 44A, 371 (1973).

⁸V. Dolat, J. B. Ross, and R. Bray, Appl. Phys. Lett. 13, 60 (1968); J. B. Ross, Ph.D thesis, Purdue University, 1972 (unpublished).

⁹H. N. Spector, Phys. Rev. 125, 1880 (1962), and 165, 562 (1968); K. P. Weller and T. Van Duzer, J. Appl.

Phys. 40, 4278 (1969); W. J. Fleming and J. E. Rowe, J. Appl. Phys. 42, 2041 (1971). The frequency of maximum acoustoelectric gain for small phonon intensity is given by $f_m = (1/2\pi)(ne^2v_s^2/kT)^{1/2}$ when the condition $q_m l / \mu B < 1$ applies, as is especially the case for the present experiment. (v_s is the fast-TA-phonon velocity, equal to 2.3×10^5 cm/sec; $q_m = 2\pi f_m / v_s$, and l and μ are the mean free path and mobility of the electrons.) The frequencies observed for the phonon satellite peaks will be generally somewhat lower than f_m because the frequency dependence of the lattice attenuation shifts the *net* gain downward (see Ref. 1). There can be further downshift with increasing phonon intensity [see T. E. Parker and R. Bray, Phys. Lett. 45A, 347 (1973)].

¹⁰General Electric No. 7031.

¹¹R. Bray, IBM J. Res. Develop. 13, 487 (1969).

¹²Parker and Bray, Ref. 9.

¹³D. G. Carlson and A. Segmüller, Phys. Rev. Lett. 28, 175 (1972).

¹⁴H. Kroger, Appl. Phys. Lett. 4, 190 (1964); E. M. Conwell and A. K. Ganguly, Phys. Rev. B 4, 2535 (1971).

¹⁵B. W. Batterman, Phys. Rev. 127, 686 (1962).

Van Hove Singularities of the Surface Phonon Density from Inelastic Reflection of Atoms*

Giorgio Benedek

*Gruppo Nazionale de Struttura della Materia del Consiglio Nazionale delle Ricerche,
Istituto di Fisica dell'Università, Milan, Italy*

(Received 19 February 1975)

The main peaks of the angular distribution of atoms inelastically reflected from a crystal surface are shown to be associated with analytical critical points of the surface phonon dispersion curves, particularly those of Rayleigh and Lucas modes. Because of such a relation, the frequencies and wave vectors of these modes could be measured by analyzing the shift of the peaks under a change of the angle of incidence.

Since the work by Cabrera, Celli, and Manson,¹ the inelastic reflection of atoms by crystal surfaces has been considered one of the most useful tools for investigating surface phonons. However, coupled high-resolution measurements of both velocity and angular distributions² are still severely limited by the actual low detection efficiencies. Williams and Mason,^{3,4} through sophisticated measurements of the angular distribution of He and Ne scattered from LiF and NaF surfaces, were able to show that the sidebands observed around the elastic peaks correspond to one-phonon inelastic processes and, in some cases, can be associated with Rayleigh waves.

In this Letter I show that the main peaks of the inelastic angular distribution, observed under suitable experimental conditions, are related to analytical critical points of the surface dispersion curves, namely to Van Hove singularities of the surface density,⁵ and particularly to those associated with Rayleigh and Lucas⁶ modes.

The differential one-phonon reflection coefficient, at zero surface temperature and up to unitarity corrections, is given by⁷

$$\frac{d^2R^{(1)}}{d\omega d\Omega_f} = \frac{m^2 \alpha_c}{4\pi^2 \hbar^3} \frac{q_f}{q_{iz}} \sum_{\gamma\gamma'} Z_{\gamma'}^*(\vec{K}, \omega) Z_{\gamma}(\vec{K}, \omega) \rho_{\gamma\gamma'}(\vec{k}, \omega^2), \quad (1)$$

where ω is the phonon frequency, Ω_f the outgoing-beam solid angle, m the particle mass, α_c the surface unit-cell area, $\vec{q}_i = (\vec{K}_i, q_{iz})$ and $\vec{q}_f = (\vec{K}_f, q_{fz})$ the wave vectors of incoming and outgoing particles,

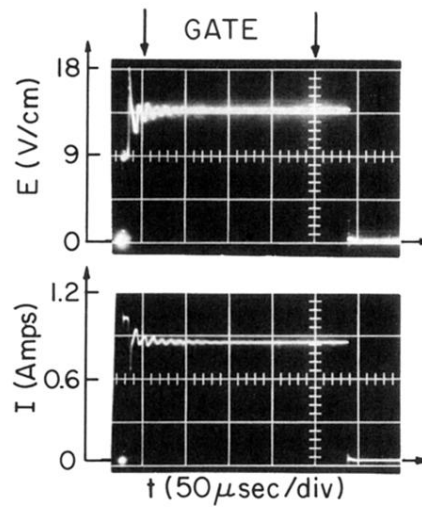


FIG. 1. Typical current and voltage pulses. After an initial Ohmic value, the building up of AE flux manifests itself through a series of damped oscillations. The steady-state regime is an indication of a stationary domain.